TIME-OF-FLIGHT CONTROL AND PASSIVE COMPRESSION IN AN α-MAGNET BEAMLINE FOR MHZ MEV UED

B. Song*, Y. Yang, P. Lv, Z. Wang, L. Zheng, Y. Du, W. Huang, C. Tang, R. Li
Department of Engineering Physics, Tsinghua University, Beijing, China

Abstract

A passive-compression beamline for high-repetition-rate MeV ultrafast electron diffraction (UED) is studied using a normal-conducting very-high-frequency (VHF) gun and a low-gradient α-magnet. The design uses the negative longitudinal dispersion of the α-magnet to compensate the positive dispersion accumulated in the gun and drift sections, while retaining a small residual total dispersion to reduce the required momentum chirp and suppress nonlinear longitudinal distortion. For near-MeV beams, the velocity-dependent contribution to R_{56}^{α} is included when setting the compression and time-of-flight (TOF) operating point. GPT simulations with CST-calculated field maps and three-dimensional space charge show that a 4.1 fC bunch can be compressed to 4.7 fs RMS at the sample, with a statistical TOF jitter of 1.9 fs RMS and normalized transverse emittances of 5.6 nm·rad and 5.2 nm·rad in the horizontal and vertical planes, respectively. These results identify controlled residual longitudinal dispersion as a practical condition for simultaneously achieving few-femtosecond compression and high timing stability in MHz-class MeV UED.

INTRODUCTION

Ultrafast electron diffraction (UED) is a powerful tool for probing structural dynamics in matter with atomic spatial resolution and femtosecond temporal resolution [1,2]. Compared with conventional keV UED systems, MeV UED benefits from reduced space-charge broadening, increased penetration depth, and improved diffraction fidelity for thicker samples [3]. These advantages make relativistic UED attractive for experiments requiring both high temporal resolution and sufficient scattering signal.

High repetition rate is also important because it improves accumulated diffraction statistics and enables measurements of weakly scattering, dose-sensitive, or irreversible processes. Normal-conducting very-high-frequency (VHF) guns operated in continuous-wave mode are promising sources for this purpose because they can provide near-MeV electron beams at MHz repetition rates with good stability and compact system integration [4].

To fully exploit such sources, the electron bunch must be compressed to the few-femtosecond regime without degrading transverse beam quality or introducing excessive arrival-time jitter. RF and THz bunchers can provide strong longitudinal phase-space rotation, but they introduce additional synchronization or high-field requirements. Passive magnetic compression avoids an externally phased field and is therefore attractive for high-repetition-rate UED. Its performance, however, is governed by the same longitudinal dispersion that determines the sensitivity of the arrival time to energy fluctuations.

An α-magnet provides a compact source of negative longitudinal dispersion and naturally generates a high-horizontal-dispersion plane that can be used for energy selection. Recent work has shown sub-5-fs compression with a high-gradient α-magnet and a low-jitter photoinjector [5]. In a VHF-gun beamline near the MeV scale, however, the positive drift dispersion and the velocity-dependent contribution inside the α-magnet are both significant. The central design problem is therefore not simply to minimize R_{56}^{tot}, but to choose a residual dispersion that enables compression while maintaining low TOF jitter.

BEAMLINE DESIGN

The proposed beamline is driven by a normal-conducting VHF gun operating at 216.7 MHz. The gun produces near-MeV electron bunches with a nominal kinetic energy of about 784 keV at the sample-side working point. The schematic layout is shown in Fig. 1. After emission from the photocathode, the beam is focused by a solenoid and passes through an upstream collimator before entering the α-magnet.

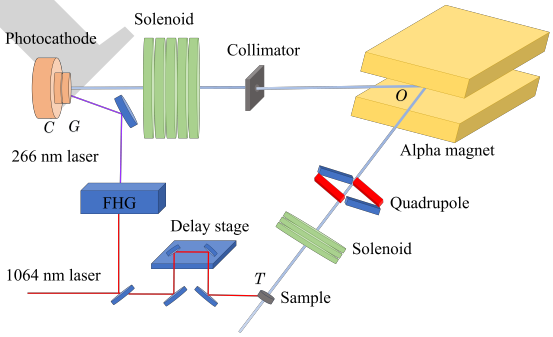

Figure 1: Schematic layout of the proposed MeV UED beamline based on a VHF gun and an α-magnet compressor.

The upstream collimator acts as a first-stage phase-space selection element. It reduces the charge density near the downstream waist, suppresses space-charge-driven nonlinear growth, and removes large-amplitude particles before the dispersive section. This cleaning is important because the following α-magnet couples transverse position, momentum deviation, and path length.

The α-magnet plays two roles. First, it provides the negative longitudinal dispersion required to rotate the longitudinal phase space and compress the bunch. Second, it produces a plane with large horizontal dispersion near the

* sbt24@mails.tsinghua.edu.cn

top of the trajectory. A slit placed at this plane removes particles with large momentum deviation and large transverse offset, thereby suppressing nonlinear longitudinal tails. A downstream quadrupole corrects the transverse asymmetry introduced by the bend, and a final solenoid matches the beam onto the sample plane.

From a beam-dynamics standpoint, compression and timing stability are coupled. Increasing the magnitude of the total longitudinal dispersion improves the phase-space rotation for a given chirp, but also increases the sensitivity of the arrival time to momentum fluctuations. The beamline is therefore optimized for a small but nonzero residual total dispersion rather than for exact first-order TOF cancellation.

LONGITUDINAL OPTICS AND COMPRESSION STRATEGY

The first-order longitudinal transport coefficient is defined as

$$R_{56} = \frac{\partial z}{\partial \delta}, \qquad \delta = \frac{\Delta p}{p}, \tag{1}$$

where z is the longitudinal coordinate relative to the reference particle and δ is the relative momentum deviation. For the near-MeV beam considered here, the drift contribution is not negligible and is approximately

$$R_{56}^{d} = \frac{d}{\gamma^2}, \tag{2}$$

where d is the drift length and γ is the Lorentz factor. The total first-order longitudinal dispersion from cathode to sample is therefore written as

$$R_{56}^{\mathrm{tot}} = R_{56}^{CG} + R_{56}^{GO} + R_{56}^{\alpha} + R_{56}^{OT}, \tag{3}$$

where the four terms correspond to the gun region, the drift from the gun exit to the α-magnet, the α-magnet itself, and the downstream drift to the sample.

For the low-gradient α-magnet, the near-MeV expression used in the design is

$$R_{56}^{\alpha} = -9.6\sqrt{\frac{\gamma\beta}{g}} + \frac{S}{\gamma^2}, \qquad S = 19.2\sqrt{\frac{\gamma\beta}{g}}, \tag{4}$$

where g is the magnetic-field gradient in T/m, β is the normalized velocity, and both R_{56}^{α} and the path length S are in centimeters. The first term represents the gradient-dependent trajectory length, while the second term accounts for the velocity-dependent delay accumulated along the finite path. This term is often negligible for highly relativistic beams, but it is important at the 0.8 MeV scale and must be included when selecting the compression working point.

If the incoming bunch has a linear chirp

$$h = \frac{d\delta}{dz}, \tag{5}$$

then the first-order longitudinal coordinate after transport is

$$z_f = \left(1 + hR_{56}^{\mathrm{tot}}\right) z_i + R_{56}^{\mathrm{tot}} \delta_{\mathrm{unc}}, \tag{6}$$

where δ_{unc} is the uncorrelated momentum spread. The linear compression condition is therefore

$$1 + hR_{56}^{\mathrm{tot}} = 0. \tag{7}$$

At the same time, momentum fluctuations generate arrival-time fluctuations according to

$$\Delta t = \frac{R_{56}^{\mathrm{tot}}}{\beta c}\,\delta. \tag{8}$$

Thus, exact cancellation of R_{56}^{tot} minimizes first-order energy-to-TOF conversion, whereas compression requires a finite product hR_{56}^{tot}. In the optimized design, the gun phase and α-magnet strength are chosen to give $R_{56}^{\mathrm{tot}} \simeq -1.57$ cm. This residual dispersion relaxes the chirp requirement, mitigates nonlinear phase-space distortion, and keeps the RF-amplitude-induced TOF response at the few-femtosecond level.

SIMULATION MODEL AND OPTIMIZATION RESULTS

Particle-tracking simulations were performed using GPT with CST-calculated electromagnetic field maps. Space-charge effects were included with the three-dimensional mesh algorithm. The beamline was optimized using a multi-objective genetic algorithm (MOGA), with the bunch duration, transverse emittance, and transmitted charge as the main performance objectives.

The resulting Pareto fronts are shown in Fig. 2. Several branches corresponding to different initial UV-laser durations were identified. The 300 fs FWHM branch was selected as the practical operating region because it provides a sufficiently strong initial momentum chirp while remaining compatible with high-repetition-rate laser operation.

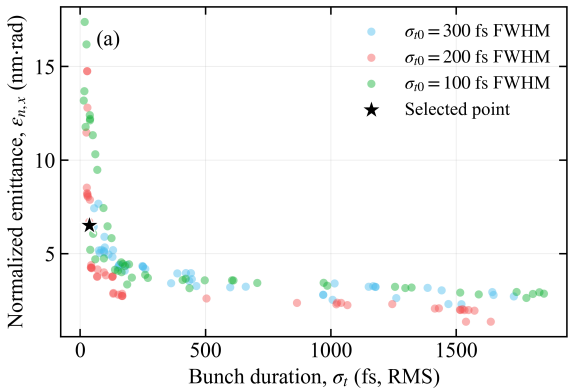

Figure 2: Pareto front obtained from the multi-objective optimization of bunch length and transverse emittance. The selected working point is taken from the 300 fs FWHM laser-duration branch.

The evolution of the main beam parameters along the local trajectory coordinate is shown in Fig. 3. The optimized beam parameters at the sample plane are summarized in Table 1. The listed principal operating point includes the energy-selecting slit; the corresponding bunch length without the slit is included to show the effect of nonlinear-tail removal.

Table 1: Optimized Beam Parameters at the Sample Plane

Parameter	Value	Unit
Beam energy	784	keV
Final bunch charge	4.1	fC
Bunch length, with slit (RMS)	4.7	fs
Bunch length, without slit (RMS)	36.7	fs
R_{56}^{tot}	−1.57	cm
TOF jitter (RMS)	1.9	fs
Norm. emittance x	5.6	nm·rad
Norm. emittance y	5.2	nm·rad

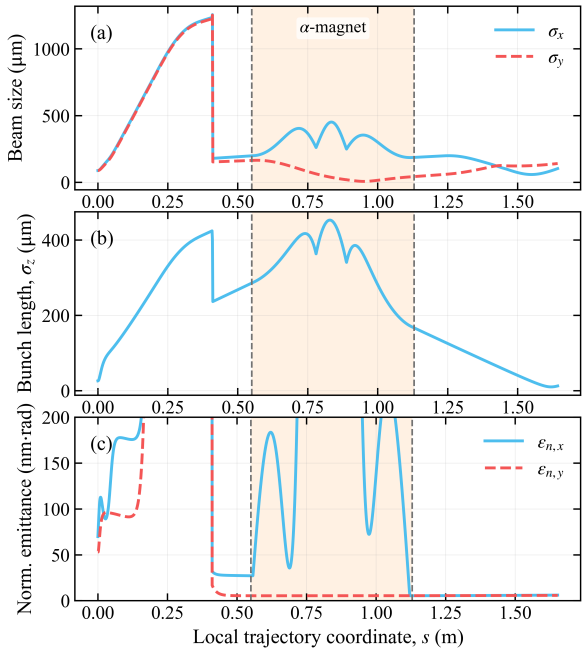

Figure 3: Evolution of the transverse beam size, longitudinal bunch length, and normalized transverse emittance along the beamline.

A 500 μm slit is placed at the high-dispersion location in the α-magnet transport. Because the horizontal coordinate at this plane is strongly correlated with momentum deviation, the slit acts as an energy-selection element. It removes nonlinear momentum tails that would otherwise dominate the final longitudinal distribution. In the selected operating point, the slit reduces the bunch duration from 36.7 fs RMS to 4.7 fs RMS at the sample.

The TOF sensitivity was evaluated using the measured VHF-gun RF amplitude jitter of 4.6×10^{-5}. The corresponding momentum fluctuation was obtained from

$$\frac{\Delta E_k}{E_k} = \frac{\gamma + 1}{\gamma} \frac{\Delta p}{p}. \tag{9}$$

For $R_{56}^{\mathrm{tot}} \simeq -1.57$ cm, the resulting path-length fluctuation is approximately 0.5 μm RMS, corresponding to a TOF jitter of about 1.9 fs RMS. Figure 4 shows the simulated arrival-time statistics for 230 consecutive shots, including RF amplitude, phase, and frequency fluctuations. The Gaussian-fitted TOF jitter is also 1.9 fs RMS, confirming that the controlled residual dispersion remains compatible with sub-10-fs timing stability.

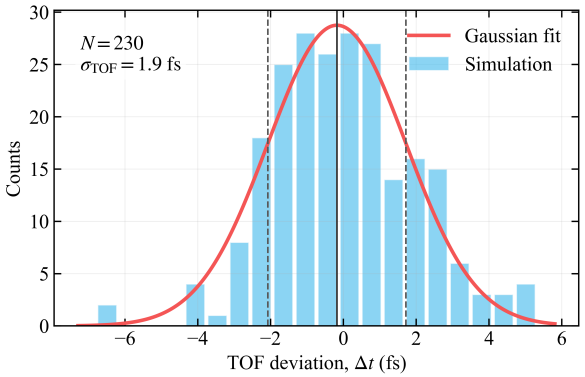

Figure 4: Simulated TOF statistics for 230 consecutive shots including RF amplitude, RF phase, and RF frequency fluctuations. The Gaussian-fitted TOF jitter is 1.9 fs RMS.

The normalized transverse emittances at the sample are preserved at 5.6 nm·rad in the horizontal plane and 5.2 nm·rad in the vertical plane. Additional robustness tests indicate that the compressed bunch length remains stable within about 2.0 fs RMS under the dominant laser and magnet jitter sources considered. These results support the selected operating point as a finite-tolerance region rather than an isolated numerical optimum.

A double-α-magnet layout was also examined as an engineering extension. This configuration restores a more linear downstream beamline geometry and allows the straight section downstream of the gun to be used for other applications when the α-magnets are switched off. It can maintain sub-10-fs compression, but the additional drift and transverse matching complexity increase the final transverse emittance. It is therefore best regarded as a construction-oriented alternative to the single-α baseline.

CONCLUSION

A passive-compression strategy for a MHz MeV UED beamline based on a VHF gun and a low-gradient α-magnet has been studied with emphasis on the coupled requirements of bunch compression and TOF stability. The near-MeV longitudinal-transport analysis shows that the velocity-dependent contribution to R_{56}^{α} should be included and that exact cancellation of R_{56}^{tot} is not necessarily the best compression operating point.

For the selected working point, the beamline retains a small residual total dispersion of about −1.57 cm. This choice reduces the chirp requirement, suppresses nonlinear longitudinal distortion, and keeps the RF-amplitude-induced TOF jitter at the few-femtosecond level. GPT simulations predict a 4.7 fs RMS bunch duration at the sample, a statistical TOF jitter of 1.9 fs RMS, and normalized transverse emittances of 5.6 nm·rad and 5.2 nm·rad. These results support α-magnet-based passive compression as a practical route toward high-repetition-rate MeV UED facilities.

REFERENCES

[1] J. B. Hastings *et al.*, "Ultrafast time-resolved electron diffraction with megavolt electron beams," *Appl. Phys. Lett.*, vol. 89, p. 184109, 2006. doi:10.1063/1.2397014

[2] D. Filippetto *et al.*, "Ultrafast electron diffraction: visualizing dynamic states of matter," *Rev. Mod. Phys.*, vol. 94, p. 045004, 2022. doi:10.1103/RevModPhys.94.045004

[3] K. M. Siddiqui *et al.*, "Relativistic ultrafast electron diffraction at high repetition rates," *Struct. Dyn.*, vol. 10, p. 064302, 2023. doi:10.1063/4.0000247

[4] L. Zheng *et al.*, "Design, fabrication, and beam commissioning of a 216.667 MHz continuous-wave photocathode very-high-frequency electron gun," *Phys. Rev. Accel. Beams*, vol. 26, p. 103402, 2023. doi:10.1103/PhysRevAccelBeams.26.103402

[5] Y. Yang *et al.*, "Sub-5-fs compression and synchronization of relativistic electron bunches enabled by a high-gradient α-magnet and low-jitter photoinjector," Aug. 2025. doi:10.48550/arXiv.2508.03946